# CrystEngComm

Accepted Manuscript






ROYAL SOCIETY OF CHEMISTRY

www.rsc.org/crystengcomm

Journal Name

RSCPublishing

ARTICLE

# Population balance model for solvent-mediated polymorphic transformation in unseeded solutions

Cite this: DOI: 10.1039/x0xx00000x

M. Kobari,[*a,c] N. Kubota[b] and I. Hirasawa[c]

Received 00th January 2012,
Accepted 00th January 2012

DOI: 10.1039/x0xx00000x

www.rsc.org/

A new population balance model for solvent-mediated polymorphic transformation was presented. The model takes into account the secondary nucleation caused by nuclei grown crystals as well as the primary nucleation. Numerical simulation was performed for crystallization of a hypothetical enantiotropic dimorphic compound in an unseeded solution. In the simulation, particular attention was paid to the effect of secondary nucleation of the stable polymorph on the transformation time. The simulated transformation time decreased with an increase in the secondary nucleation rate of the stable polymorph. Reported experimental data on the effect of stirrer speed was explained with the secondary nucleation-mediated mechanism, in which the secondary nucleation rate was assumed to increase with an increase in stirrer speed. The effect of scale-up on the transformation time was also suggested to be explained with the secondary nucleation-mediated mechanism.

## Introduction

Clarifying polymorphism is very important in the pharmaceutical and fine chemical industries. Diverse polymorphs have differences in physical properties, such as crystal habit, solubility, hardness, colour, optical properties, melting point and chemical reactivity[1]. Polymorphism has a significant effect on the performance of the products. It depends on the operating conditions such as seeding, agitation rate[2,3,4,5,6,7] reactor size[3,4], temperature[8], concentration, the presence of impurities[9,10] and seeding.[2,7,8,10,11,12,13,14,15,16,17,18] Polymorphism sometimes shows unexpected behaviour in an industrial crystallizer[19].

A metastable polymorph (high solubility) transforms into a lower solubility polymorph during crystallization with the solvent - mediated[2,5,6,8,13,14,15,17,20,21] (or solution - mediated[1,3,4,7,9,12,16,22,23,24,25,26]) mechanism, where the unstable polymorph crystals dissolve and the stable polymorph crystallizes. In an investigation of the mechanism of solvent-mediated polymorphic transformation, numerical simulation is a powerful tool, as it provides useful information that cannot be obtained in actual experiments. However, the reported simulation studies[2,11,13,15,17,20,23] are not satisfactory. One reason for this may be that crystallization of a polymorphic compound is very complicated, with many rate processes. Even in the simplest case of a dimorphic system, in which two polymorphs are involved, there are at least seven rate processes; primary nucleation, secondary nucleation and crystal growth for each polymorph, and dissolution of an unstable (high solubility) polymorph. It is difficult to take into account of all these rate processes properly in modelling due to a lack of information on these rate processes. In particular, it is difficult to treat nucleation processes appropriately. In some cases of unseeded solutions[5,24,25], only homogeneous primary nucleation was assumed to occur. For seeded systems[11,13,17] primary nucleation was sometimes ignored. As far as secondary nucleation is concerned, two different mechanisms have been considered. One is a surface secondary nucleation, the nucleation of the stable polymorph on the surface of the dissolving unstable polymorph.[2,4,9,12,16,17,21,22,26] This type of secondary nucleation was first observed by Davey et al.[3], using an electron microscope, for the polymorphic crystallization of 2,6-dihydroxybenzoic acid in chloroform. Davey et al. also reported, in the same paper[3], that ordinary secondary nucleation, which is a well-known phenomenon[28] in non-polymorphic suspension crystallization, play a dominant role in the solvent-mediated transformation.[7] This is another type of secondary nucleation. Hermanto et al.[11] and Ono et al.[13] employed independently the mechanism of ordinary secondary nucleation of a stable polymorph for simulations of polymorphic transformation in seeded solutions. However, the ordinary secondary nucleation of an unstable polymorph has never been considered in simulation studies up to now.

In this study, a new population balance model for solvent-mediated polymorphic transformation in unseeded solutions is presented, in which the ordinary secondary nucleation caused by nuclei grown crystals and primary nucleation are both taken into account. This model can be extended easily to seeded

systems by changing the initial conditions. This model is applied to simulate a hypothetical dimorphic system, and the effects of stirrer speed and vessel size (or scale-up) on the transformation time is analysed. The aim of this paper is to propose a theoretical framework of the solvent-mediated polymorphic phase transformation.

## Population balance model

A batch unseeded cooling crystallization process of a multi-polymorphic system in a perfectly-mixed crystallizer can be modelled and described as follows. There are multiple assumptions made in the mathematical formulation. First, crystal growth rate is independent of crystal size (McCabe's $\Delta L$ law[30]) and dissolution rate of crystal does not depend on crystal size. There is no account for crystal breakage, crystal agglomeration or crystal growth rate dispersion[28,30].The population balance equation (PBE)[11,13,15,17,22] for a polymorph $i$ is given as

$$\frac{\partial n_i(L_i,t)}{\partial t} + G_i \frac{\partial n_i(L_i,t)}{\partial L_i} = \left(B_{1,i} + B_{2,i}\right)\delta(L_i - L_{0,i}) \qquad (i = \alpha, \beta, .....) \tag{1}$$

Here, $n_i(L_i,t)$ is the population density function of the total crystals present in the crystallizer, $t$ is the time, $L_i$ is the characteristic length of crystal. $G_i$ (=d$L_i$/d$t$) is the linear growth rate of stable polymorph crystal or the linear dissolution rate of unstable polymorph crystal. $B_{1,i}$ is the rate of primary nucleation, $B_{2,i}$ is the rate of secondary nucleation of stable polymorph and $\delta(L_i\text{-}L_{0,i})$ is Dirac's delta function ($\delta(L\text{-}L_{0,i}) = \infty$ at $L = L_0$ and $\delta(L\text{-}L_{0,i}) = 0$ at $L \neq L_{0,i}$ with $\int_{-\infty}^{+\infty}\delta(x)dx = 1$).[31] $L_{0,i}$ is the size of nucleus, which is assumed to be the same size, regardless of primary or secondary nucleation. These assumptions lead to simple mathematical formulation and easy calculation without misjudging the nature of polymorphic crystallization.

The mass balance can be written with the following equation as

$$\frac{\mathrm{d}C}{\mathrm{d}t} = -\sum_i \rho_{c,i} k_{v,i}\left\{3G_i\mu_{2,i} + \left(B_{1,i} + B_{2,i}\right)L_{0,i}^3\right\} \qquad (i = \alpha, \beta, .....) \tag{2}$$

where $C$ is the solution concentration, $\rho_{c,i}$ is the density of the crystals and $k_{v,i}$ is the shape factor of the crystals. As there are no crystals of any size at the start of the simulation, the initial conditions are given as

$$n_i(L_i,0) = 0 \tag{3}$$

and

$$C(0) = C_0 \tag{4}$$

where $C_0$ is the initial concentration.

The moment method[16,23] was employed to solve simultaneously the PBE and the mass balance equation. The $j$-th order moment of crystal size distribution is defined as

$$\mu_{j,i} = \int_0^\infty L^{j,i} n_i(L_i,t)dL_i \tag{5}$$

Eqn (1) is transformed to the following set of ordinary differential equations:

$$\frac{d\mu_{0,i}}{dt} = B_{1,i} + B_{2,i} \tag{6}$$

$$\frac{d\mu_{j,i}}{dt} = jG\mu_{j-1,i} + \left(B_{1,i} + B_{2,i}\right)L_{0,i}^j \qquad j = 1, 2, \cdots \tag{7}$$

And the initial condition of eqn. (3) was transformed to

$$\mu_{j,i}(0) = 0 \qquad j = 0, 1, 2, \cdots \tag{8}$$

For a given cooling profile, the moment $\mu_{j,i}$ and the solution concentration $C$ can be obtained as a function of time by solving eqns (2), (6) and (7) numerically and simultaneously with the initial conditions of eqns (4) and (8), if the kinetics of primary and secondary nucleations and growth and the solubilities of all polymorphs are known.

The primary nucleation rate per unit mass of solvent is assumed to be expressed for stable and unstable polymorph, respectively, by

$$B_{1,i} = \begin{cases} k_{b1,i}\left(\Delta T_i\right)^{b1_i} & 0 \le \Delta T_i \\ 0 & \Delta T_i < 0 \end{cases} \tag{9}$$

where $k_{b1,i}$ and $b1_i$ are the empirical constants and $\Delta T_i$ is the supercooling. It is defined as

$$\Delta T_i = T_{sat,i} - T \tag{10}$$

where $T_{sat,i}$ is the saturation temperature and $T$ is the solution temperature. The secondary nucleation rate $B_{2,i}$ is assumed to be given by the following equation:

$$B_{2,i} = \begin{cases} k_{b2,i}\left(\Delta T_i\right)^{b2_i}\mu_{3,i} & 0 \le \Delta T_i \\ 0 & \Delta T_i < 0 \end{cases} \tag{11}$$

where $k_{b2,i}$ is the secondary nucleation rate constant, $b2_i$ is the secondary nucleation order and $\mu_{3,i}$ is the third moment of crystal size distribution, with which the effect of the magma density of the crystals (*i.e.*, mass density of each polymorph present in the solution) on the rate of secondary nucleation is considered. It must be noted that the rate of secondary nucleation is known to increase linearly with an increase in magma density.[28] The overall nucleation rate is assumed to be given with the sum of the primary and secondary nucleation rates for each polymorph as

$$B_i = B_{1,i} + B_{2,i} = k_{b1,i}(\Delta T_i)^{b1_i} + k_{b2,i}(\Delta T_i)^{b2_i}\mu_{3,i} \quad (12)$$

To formulate the solvent-mediated polymorphic transformation process, dissolution of unstable polymorph $i$ should be considered. During dissolution, unstable polymorph crystals decrease in size with time and finally disappear at the nucleus size $L_0$. However, the number rate of disappearance is impossible to predict, because the number of nuclei (*i. e*., the number of crystals of size $L_0$) or crystal size distribution is not known as long as the moment method is employed. The moment method deals with only the moments of crystal size distribution. As already described in eqns (9) and (11), the number rate of disappearance of unstable polymorph was assumed to be zero ($B_i = B_{1,i} + B_{2,i} = 0$).[2,23,31] This is an inevitable assumption. It has little influence on the term ($B_{1,i} + B_{2,i}$)$L_{0,i}^3$ of the right hand side of eqns (2) and (7), because the size of nuclei $L_0$ itself is very small. However, the second moment $\mu_{2,i}$ for unstable polymorph $i$ remains constant, and, therefore, the term $3G_i\mu_{2,i}$ in eqn (2) and eqn (7), which is negative due to $G_i < 0$, does not varnish numerically. This produces a serious effect on the formation of the stable polymorph crystals; the term $3G_i\mu_{2,i}$ in eqn (2) for stable polymorph continues to increase due to mass balance constraint and the third moment $\mu_{3,i}$ (or mass) of the stable polymorph continues to increase to infinity according to eqn (7). This is unrealistic. To avoid this problem, a factor $f_i$ was introduced into eqns (2) and (7); the terms $3G_i\mu_{2,i}$ and $jG_i\mu_{j\text{-}1,i}$ were replaced by $3f_iG_i\mu_{2,i}$ and $f_ijG_i\mu_{j\text{-}1,i}$ respectively, during dissolution at $\Delta T_i < 0$. The factor $f_i$ is defined as

$$f_i \equiv \frac{\mu_{3,i}}{\mu_{3,i}(t_A)} \quad (13)$$

where $\mu_{3,i}$ is the third moment of size distribution of unstable polymorph during dissolution and $\mu_{3,i}(t_A)$ is the value of $\mu_{3,i}$ at the start of dissolution (or at the start of solvent-mediated transformation). The time $t_A$ is the time at the start of transformation. The factor $f_i$ is the remaining mass ratio of unstable polymorph crystals. By this, the rate of dissolution of unstable polymorph is gradually lowered and dissolution ceases finally at $f_i = 0$. Thus, the above mentioned unrealistic behaviour of dissolution of unstable polymorph can be avoided.

The growth and dissolution rates are given as

$$G_i = \begin{cases} k_{g,i}(\Delta T_i)^{g_i} & 0 \le \Delta T_i \text{ (growth)} \\ -k_{d,i}(-\Delta T_i)^{d_i} & \Delta T_i < 0 \text{ (dissoluti on)} \end{cases} \quad (14)$$

where $k_{g,i}$, $k_{d,i}$, $g_i$ and $d_i$ are the empirical constants and $-\Delta T_i$ is the undercooling ($T - T_{sat}$). As in eqn (14), the growth rate is assumed to be proportional to the $g_i$-th power of the supercooling, while the linear dissolution rate $G_i$ (=d$L_i$/d$t$ < 0), which is negative growth rate, is assumed to be proportional to the $d_i$-th power of undercooling and the third moment of crystal size distribution.

## Simulation for an enantiotropic dimorphic system

Simulation of the solvent-mediated polymorphic transformation was performed for an unseeded solution of a hypothetical dimorph.

### Solubility curves

Solubility curves of a dimorphic hypothetical compound are shown in Fig. 1. The solubility curves cross at 43.9 °C. Below this temperature, polymorph $\alpha$ is unstable and polymorph $\beta$ is stable; whereas, above this transition temperature, the stability is reversed. This system is enantiotropic. The solubilities of polymorphs $\alpha$ and $\beta$ are described mathematically with second-order polynomials, respectively as

$$C_{sat,\alpha} = 1.532\times10^{-1} - 4.215\times10^{-3}T + 9.411\times10^{-5}T^2 \quad (15)$$

and

$$C_{sat,\beta} = 1.414\times10^{-1} - 5.513\times10^{-3}T + 1.298\times10^{-4}T^2 \quad (16)$$

where $C_{sat,\alpha}$ is the solubility of polymorph $\alpha$, $C_{sat,\beta}$ is that of polymorph $\beta$ and $T$ is the solution temperature in Celsius. The solubilities of polymorphs $\alpha$ and $\beta$ are both assumed to be independent of crystal size.

The saturation temperatures of polymorphs $\alpha$ and $\beta$, $T_{sat,\alpha}$ and $T_{sat,\beta}$ (in Celsius) of a solution at concentration $C$ are calculated by using the following equations, respectively.

$$T_{sat,\alpha} = 22.394 + (-1126.4 + 10626\,C)^{\frac{1}{2}} \quad (17)$$

$$T_{sat,\beta} = 21.237 + (-638.40 + 7704.2\,C)^{\frac{1}{2}} \quad (18)$$

These equations are the inverse functions of the solubility curves eqns (15) and (16), respectively.

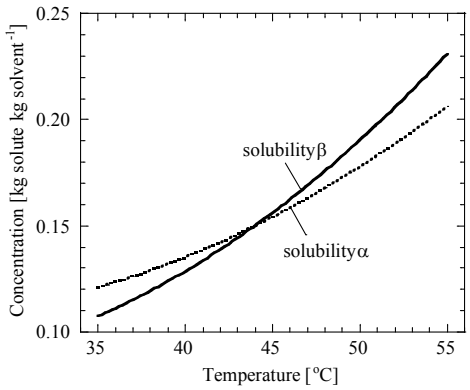


**Fig. 1** Solubilities of polymorphs α and β of a hypothetical polymorphic compound.

### Temperature profile

The cooling profile used in this study is defined in Fig. 2. The temperature was lowered first at a constant rate of 0.167 °C/min (10 °C/h) from 55 °C to 35 °C and then it was kept constant at 35 °C for 8 hours.

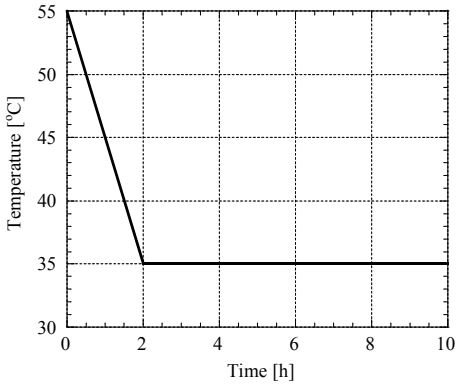


**Fig. 2** Cooling profile for solvent-mediated polymorphic transformation, combined polythermal and isothermal conditions.

### Simulation conditions

The parameters used for the simulation are listed in Table 1. The values of these parameters were set to be the same for both polymorphs $\alpha$ and $\beta$. This set is a standard. To explore the mechanism of transformation, the primary nucleation rate constant $k_{b1,\beta}$ was set from $1\times10^{-7}$ to $1\times10^{-5}$, and the secondary nucleation constant $k_{b2,\beta}$ was varied over a wide range: $k_{b2,\beta}=1\times10^{2} \sim 1\times10^{6}$.

The calculation was carried out with MATLAB (R2007b).

**Table 1** Parameter values used as a standard for simulation.

| parameters | values(form $\alpha$) | values(form $\beta$) | upunits |
|---|---|---|---|
| $k_{b1,i}$ | $1\times10^{-7}$ | $1\times10^{-7}$ | $s^{-1}$ kg solvent$^{-1}$ °C$^{-b1,i}$ |
| $b1_i$ | 6 | 6 | - |
| $k_{b2,i}$ | $1\times10^{5}$ | $1\times10^{5}$ | $s^{-1}$ kg solvent$^{-1}$ °C$^{-b2,i}$ |
| $b2_i$ | 2 | 2 | - |
| $k_{g,i}$ | $1\times10^{-7}$ | $1\times10^{-7}$ | m $s^{-1}$ °C$^{-gi}$ |
| $g_i$ | 1 | 1 | - |
| $L_{0,i}$ | $1\times10^{-6}$ | $1\times10^{-6}$ | m |
| $k_{v,i}$ | 1 | 1 | - |
| $\rho_{c,i}$ | $1\times10^{3}$ | $1\times10^{3}$ | kg $m^{-3}$ |
| $k_{d,i}$ | $8\times10^{-7}$ | - | m $s^{-1}$ °C$^{-di}$ |
| $d_i$ | 1 | - | - |

## Results and discussion

### Solution and solid concentration profiles

In Fig. 3 the solution concentration numerically obtained is shown as a function of time for the parameters of the standard set in Table 1. In this figure, the solubilities of polymorphs $\alpha$ and $\beta$ are indicated with thin dashed and solid lines, respectively. After the start of cooling, solution concentration remains unchanged for about 1 hour. Then it begins to decrease, approaching the solubility of polymorph $\alpha$. At the moment when the solution concentration coincides with the solubility of polymorph $\alpha$ (vertical line A), the crystals of polymorph $\alpha$ begins to dissolve.

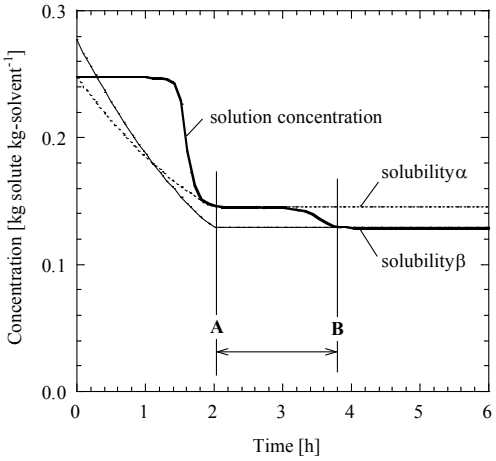


**Fig. 3** Solution concentration as a function of time. Thin dashed and solid lines are the solubilities of polymorphs $\alpha$ and $\beta$, respectively. Parameters used are listed in Table 1.

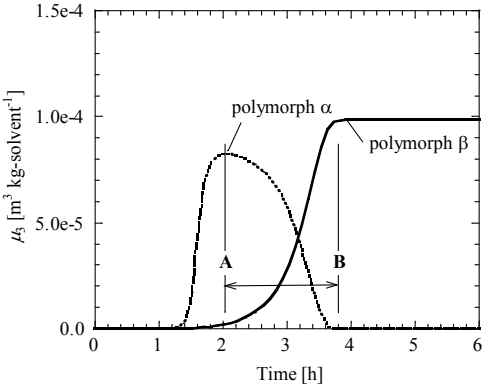


**Fig. 4** Third moments of polymorphs $\alpha$ and $\beta$ during the transformation process as a function of time. Parameters used are listed in Table 1.

Fig. 4 shows the third moments of polymorphs $\alpha$ and $\beta$ as a function of time. The third moment $\mu_{3,\alpha}$ of the size distribution of polymorph $\alpha$ crystals begins to decrease (i. e., polymorph $\alpha$ crystals begin to dissolve) at point A (The third moment multiplied by the volume shape factor $k_v$ and the solid density $\rho_c$ is the mass of $\alpha$ crystals per unit mass of solvent.). Point A is the start of the solution-mediated transformation to the stable polymorph $\beta$. The transformation continues until the solution concentration reaches the solubility of the stable polymorph $\beta$. The end point of the transformation is indicated by the vertical line B in both, Fig. 3 and Fig. 4. It is defined as the point at which the solution concentration reaches a value larger than the solubility of the stable polymorph $C_\beta$ by 2% of the solubility difference ($C_\beta$-$C_\alpha$) at the final temperature (35°C). The concentration variation in Fig. 3 exhibits a typical solvent-mediated polymorphic transformation process; the solution

concentration plateau is seen after the start of dissolution of the unstable polymorph $\alpha$. During the plateau region, the mass rate of dissolution of unstable polymorph $\alpha$ and the mass rate of crystallization (nucleation plus growth) of stable polymorph $\beta$ are balanced, as described as

$$\frac{dC}{dt} = -\rho_{c,\alpha} k_{v,\alpha} 3 G_\alpha f_\alpha \mu_{2,\alpha} - \rho_{c,\beta} k_{v,\beta} 3 G_\beta \mu_{2,\beta} = 0 \qquad (19)$$

This is a mass balance equation applied to the dimorphic system, in which the effect of mass of nuclei was ignored. The first term of the right hand of eqn (19) is the mass dissolution rate (positive, due to $G_\alpha < 0$) and the second term is the mass crystallization rate (negative, due to $G_\beta > 0$). At the final stage of transformation, the solution concentration begins to decrease and approaches the solubility of the stable polymorph $\beta$. The crystallization of $\beta$ in this stage is not balanced with the dissolution of $\alpha$. The mass crystallization rate of $\beta$ dominates the mass dissolution rate of $\alpha$ and hence the concentration of the solution decreases (*i. e.*, $dC/dt < 0$). The transformation time (the length between lines A and B in Fig. 3 and Fig. 4) is prolonged with an increase in the mass of $\alpha$ crystallized before the start of transformation and it is also prolonged with a decrease in the crystallization rate of $\beta$.

The same solution concentration variation as that in Fig. 3 is shown in a different way in Fig. 5 as a function of temperature, together with the solubility curves of polymorphs $\alpha$ and $\beta$. The solution concentration remains unchanged from the start of cooling (55°C) to about 42 °C. Then it begins to decrease and finally reaches the solubility of polymorph $\alpha$ at 35 °C. This point on the solubility curve at 35 °C corresponds to the plateau concentration in Fig. 3. The concentration drops to the solubility of polymorph $\beta$ at 35 °C.

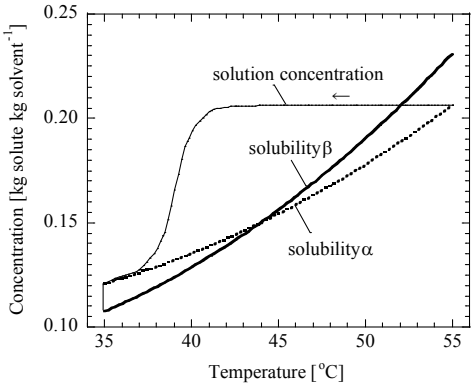


**Fig. 5** Trajectory of solution concentration together with the solubility curves of polymorphs $\alpha$ and $\beta$. Parameters used are listed in Table 1. An arrow denotes the direction of time.

**Solid composition and supersaturation profile**

Fig. 6 shows the solid compositions of polymorphs α and $\beta$ as a function of time, where lines A and B denotes the beginning and end of the transformation, respectively. The solid composition lines of $\alpha$ and $\beta$ are symmetrical with respect to the horizontal line at 50 %, simply because only these two types of polymorphic crystals are present. Before the start of the transformation at point A, the change in the solid composition is governed by the relative crystallization kinetics of the $\alpha$ and $\beta$ polymorphs with no dissolution. Once the solvent-mediated transformation starts, the dissolution process of polymorph $\alpha$ crystals begins to have an effect on the composition change.

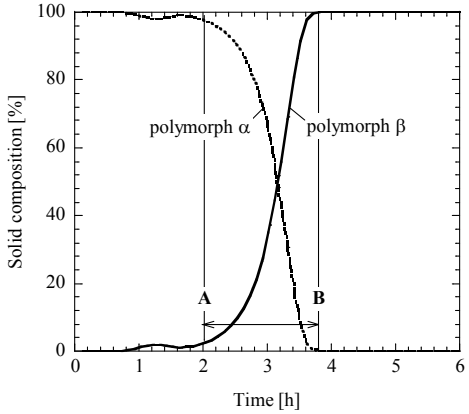


**Fig. 6** Polymorphic solid compositions as a function of time. Parameters used are listed in Table 1.

As a whole, the composition of polymorph $\alpha$ crystals decreases (and composition of polymorph $\beta$, increases) continuously with time. However, there can be seen, at $t$ = 1.2 h, before the transformation starting point A, a small irregular rise in the composition of polymorph $\alpha$ (and a corresponding small fall in the composition of polymorph $\beta$).

This irregularity is considered to be caused by the reversed crystallization rate due to the change in the magnitude of supersaturation from $\Delta C_\alpha > \Delta C_\beta$ to $\Delta C_\alpha < \Delta C_\beta$ (see Fig. 7). However, this early stage irregularity does not have any serious effect on the whole process of the composition change, because the amount of crystals is very small at this stage (see Fig. 4).

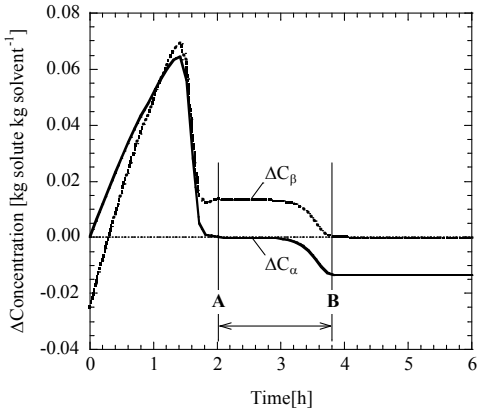


**Fig. 7** Supersaturation as a function of time. Parameters used are listed in Table 1.

In Fig. 7, the supersaturations $\Delta C_\alpha$ and $\Delta C_\beta$ for polymorphs $\alpha$ and $\beta$ respectively, are shown as a function of time. The

supersaturations increase first by cooling and, passing through the maximum, decease by crystallization (nucleation plus growth) of both polymorphs, until the start of transformation (point A). The supersaturation $\Delta C_\alpha$ decreases down to and reaches zero. Then, it remains there for a while (during the plateau region in Fig. 3) and finally decreases again to a negative value, which corresponds to the concentration saturated with respect to the solubility of polymorph $\beta$. The supersaturation $\Delta C_\beta$ also decreases from the maximum point. It decreases down to, and remains at, a certain value of supersaturation for a while. This supersaturation corresponds to the solubility of the stable polymorph $\alpha$.

It is interesting to note that there can be seen, just before the start of the transformation (point A), a small rise following a dip on the supersaturation curve of polymorph $\beta$. This is not due to the increase in the concentration by dissolution of crystals because dissolution itself never occurs before the transformation starting point A. The appearance of the rise following the dip is caused by the dominance of the rate of supersaturation creation by cooling over the overall crystallization rate of polymorphs $\alpha$ and $\beta$. Davey et al.[3] observed experimentally a similar small rise following a dip in supersaturation prior to the start of the solvent-mediated polymorphic transformation. They explained in a different way that this phenomenon was due to the supersaturation creation by dissolution of unstable polymorph crystals.

**Nucleation during the solvent-mediated transformation**

As noted above, the solution concentration profile in Fig. 3 exhibits a typical solvent-mediated polymorphic transformation process; the plateau of concentration appears prior to the final concentration fall to the solubility of the stable polymorph $\beta$. The transformation starts at the point of A and ends at the point of B. During the transformation, the unstable polymorph $\alpha$ crystals dissolve, while the stable polymorph $\beta$ crystals nucleate and grow. It is interesting to know which mechanism of nucleation, primary or secondary nucleation, dominates during the transformation. Fig. 8 shows the number densities of grown primary nuclei and grown secondary nuclei as a function of time for three different primary nucleation rates. At the lowest primary nucleation rate with $k_{b1,\beta} = 1\times10^{-7}$ s$^{-1}$ kg solvent$^{-1}$ $^{o}$C$^{-b1}$, which is the same primary nucleation rate as that used for the above standard simulations, above, (Fig. 3 to Fig. 7), crystals generated during the transformation are almost all secondary nuclei grown crystals (Fig. 8a). As the primary nucleation rate is increased to 10 times (Fig. 8b) or 100 times (Fig. 8c) higher level, the following changes are observed: (1) Primary nuclei grown crystals increase in number, while secondary nuclei grown crystals decrease in number. (2) The total number of primary and secondary nuclei grown crystals increased (not shown in Fig. 8). (3) The number ratio of primary nuclei grown crystals to secondary nuclei grown crystals increased (not shown in Fig. 8). (4) The transformation starts earlier (the position of line A moves left) and the transformation time (the length between lines A and B) becomes shorter. These changes are due to an increase in the overall growth rate of the $\beta$ polymorph caused by the increased number of the stable polymorph $\beta$ crystals. (5) The secondary nucleation of the stable polymorph $\beta$ is always dominant over the primary nucleation, over the range of parameters considered.

**The effects of agitation on transformation time**

The solvent-mediated polymorphic transformation time is known to be affected by agitation or stirrer speed.[2,3,4,5,6,7] The effect of agitation is incorporated in the present model through the kinetic constant of secondary nucleation $k_{b2,\beta}$ because the rate of secondary nucleation is considered to increase in proportion to the $j$-th power of agitation speed $N_r$ as is widely accepted[28,29,32] for non-polymorphic compounds as

$$k_{b2,\beta} \propto N_r^j \qquad (20)$$

where the exponent $j$ is an empirical constant. The value of the exponent $j$ is reported to be $j \approx 3$[28] The secondary nucleation constant $k_{b2,\beta}$ was changed over a range from $1\times10^2$ to $1\times10^6$ s$^{-1}$ kg solvent$^{-1}$ $^{o}$C$^{-b2}$. This range of the parameter $k_{b2,\beta}$ may be wider than values that would physically be expected. However, it was employed intentionally to show clearly the effect of $k_{b2,\beta}$ on the solvent-mediated polymorphic transformation.

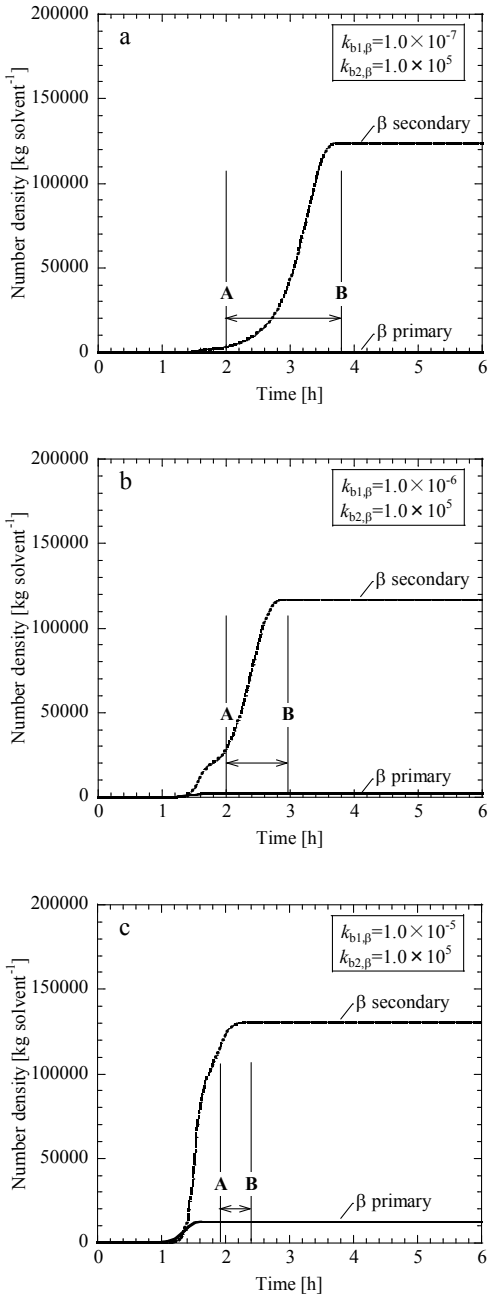


**Fig. 8** Polymorphic solid compositions at three different primary nucleation rates as a function of time: (a) low, (b) intermediate (10 times larger) and (c) high (100 times larger) primary nucleation rates.

The effect of the kinetic constant of secondary nucleation $k_{b2,\beta}$ on the simulated solution concentration is shown in Fig. 9 as a function of time with $k_{b2,\beta}$ as a parameter. As the secondary nucleation constant $k_{b2,\beta}$ is increased, the start of transformation is accelerated. At the highest secondary nucleation constant of $k_{b2,\beta}$=1×10$^6$, the transformation starts before the cooling is stopped, and the plateau region disappears. Thus, the secondary nucleation constant clearly affects the solvent-mediated polymorphic transformation. This is because the secondary nucleation dominates over the primary nucleation, as noted above.

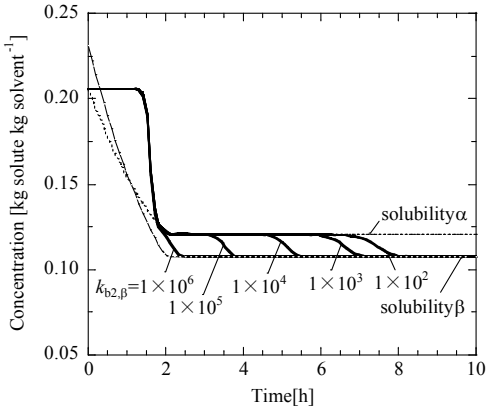


**Fig. 9** Effect of the secondary nucleation constant $k_{b2,\beta}$ on the solution concentrations during the transformation process as a function of time.

Fig. 10 shows the corresponding solid concentration profiles of polymorphs $\alpha$ and $\beta$ with the secondary nucleation constant $k_{b2,\beta}$ as a parameter. The peak of solid concentration curve of polymorph $\alpha$, which is the starting point of the dissolution of the unstable polymorph $\alpha$ crystals (or the starting point of the solvent-mediated transformation), does not move, except for the case of the highest value of $k_{b2,\beta}$ = 1×10$^3$ s$^{-1}$ kg solvent$^{-1}$ $^oC^{-b2,\beta}$. At the highest $k_{b2,\beta}$, it moves left slightly. However, the solid concentrations of both, the unstable and stable polymorphs, begin to increase almost at the same time.

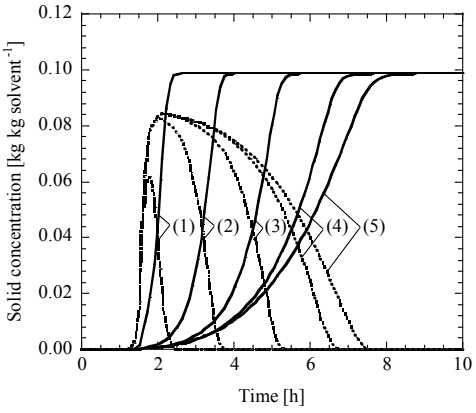


**Fig. 10** Solid concentrations of polymorph $\alpha$ and $\beta$ during the transformation process over a wide range of the secondary nucleation rate constant of polymorph $\beta$ ; $k_{b2,\beta}$ = (1) 1×10$^6$, (2) 1×10$^5$, (3) 1×10$^4$, (4) 1×10$^3$, (5) 1×10$^2$ s$^{-1}$ kg solvent$^{-1}$ $^oC^{-b2,\beta}$. Dotted lines and solid lines denote polymorph $\alpha$ and polymorph $\beta$, respectively.

In Fig. 11, the transformation time $t_{trans}$ is plotted as a function of the secondary nucleation constant $k_{b2,\beta}$ of polymorph $\beta$. The transformation time was defined and calculated with the following equation.

$$t_{trans} = t_B - t_A \quad (21)$$

where $t_A$ is the time at which the transformation starts (point A in the previous figures) and $t_B$ is the time at which the transformation ends, as defined previously. The relationship between $t_{trans}$ and $\log k_{b2,\beta}$ is seen to be linear with a negative slope. The line drawn in Fig. 11 is a best fit to the simulated data, which is

$$t_{trans} = 9.26 - 0.64 \log k_{b2,\beta} \quad (22)$$

This is an empirical equation based on the simulated results. As described above eqn (20), the secondary nucleation constant $k_{b2,\beta}$ increases in proportion to the $j$-th power of stirrer speed $N_r$. Substituting eqn (20) into (22) gives the following equation, which correlates the transformation time $t_{trans}$ with stirrer speed

$$t_{trans} = a - b \log N_r \quad (23)$$

where $a$ and $b$ are empirical constants. Experimental data of the transformation time are expected to obey eqn (23).

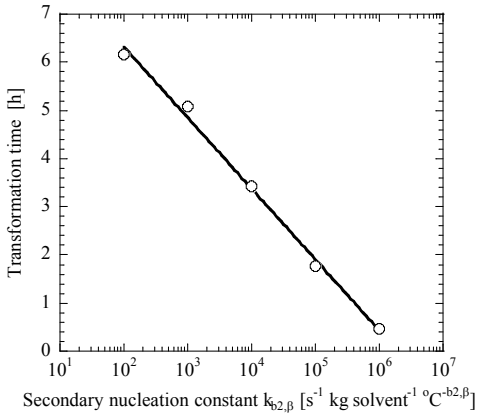


**Fig. 11** Transformation time as a function of the secondary nucleation constant $k_{b2,\beta}$.

Only a few data have been reported on the effect of stirrer speed on the transformation time. Maruyama et al.[6] studied the solvent-mediated transformation of taltireline, a central nervous system activating agent, which is an enantiotropic dimorph of polymorphs $\alpha$ and $\beta$. They measured the solid composition (or mass fraction $X_\beta$) and the solution concentration with time. Typical data are shown in Fig. 12.

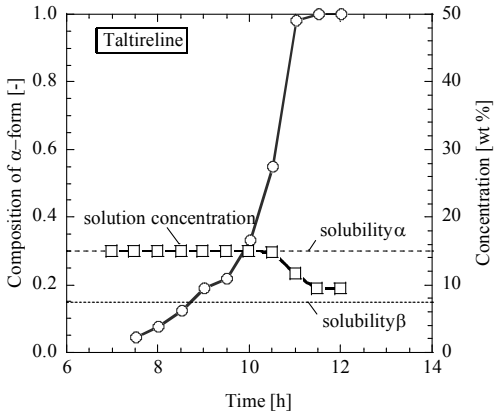


**Fig. 12** Solvent-mediated transformation of taltireline in water at 10 °C. Data were taken from Maruyama et al.[6]

The solid concentration and the mass fraction are similar to the simulated results described above. Maruyama et al.[6] obtained a linear relationship between $X_\beta^{1/3}$ with the elapsed time $t$ as

$$\sqrt[3]{X_\beta} = \frac{k_T}{3}(t - \theta) \quad (24)$$

where the constant $\theta$ is the time elapsed at the point at which the transformation starts, and $k_T$ is an experimental constant. The time $\theta$ corresponds to $t_A$ in this study. The time $t$ at $X_\beta = 1$ is the time when the transformation is complete, which corresponds to $t_B$ in this study. Therefore, the time difference ($t - \theta$) at $X_\beta = 1$ is the transformation time $t_{trans}$, which can be calculated if the constant $k_T$ is known. Transformation times for taltireline in water were calculated by using the value of $k_T$ reported by Maruyama et al.[6] The calculated results are shown in Fig. 13.

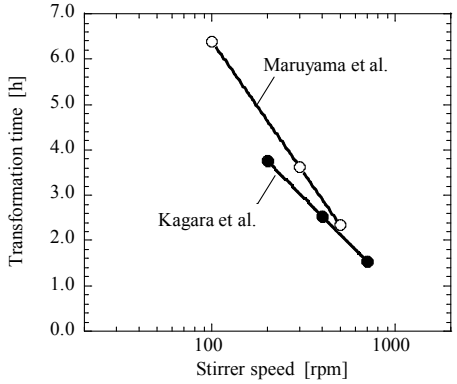


**Fig. 13**. Experimental relationships between transition time and stirrer speed for taltireline in water (Maruyama et al.[6]) and tetralin in a mixed solvent of isopropyl alcohol and water (Kagara et al.[5]). Lines are best fits of eqn (23).

The linear (solid) line is a best fit of eqn (23). Kagara et al.[5] studied the polymorphic transformation of a tetralin compound, (+)-2, 2-dibutyl-5-(2-quinolylmerthoxy)-1,2,3,4-tetrahydro-1-naphthol, in a mixed solvent of isopropyl alcohol and water,

using the same method as that used by Maruyama et al.[6] Transformation times were calculated similarly by using the values of $k_T$ reported by Kagara et al.[5] The results are also plotted in Fig. 13. The linear (solid) lines are both best fits of eqn (23). These two sets of data, which obey eqn (23), look to support the view that the transition time is affected by stirrer speed via the secondary nucleation-mediated mechanism, in which the grown crystals of the stable $\beta$ polymorph play a major role. Experimental facts that the transformation time decreases with an increase in stirrer speed have also been reported elsewhere.[2,3,4]

The plateau is not observed in Fig. 9 for the highest secondary nucleation rate, with $k_{b2,\beta} = 1\times10^6$ s$^{-1}$ kg solvent$^{-1}$ $^oC^{-b2,\beta}$. It is interesting to note that the polymorphic transformation was occurring even in this case. Therefore, it is dangerous to conclude, from the absence of the plateau in the concentration vs. time curve, that no polymorphic transformation has occurred.

**The effect of vessel volume on transformation time**

The transition time is experimentally known to increase with an increase in the vessel volume.[3,4,12,27] This scale-up effect is important in engineering practice. The scale up effect on secondary nucleation kinetics for non-polymorphic substances had been studied extensively in the past up to 1970s. Garside and Davey[28] summarized the published data in 1980 and presented an equation correlating secondary nucleation rate and crystallizer size. It can be rewritten for the rate constant of secondary nucleation of stable polymorph $\beta$ as

$$k_{b2,\beta} \propto \lambda^d \qquad (25)$$

where $\lambda$ is the length scale of a crystallizer and $d$ is an experimental constant, which characterizes the scale up effect. The value of $d$ depends on the scale up criterion. The value of $d$ is negative, if constant stirrer tip speed or stirrer speed to just maintain all crystals in suspension is assumed as a scale up criterion.[28] Recently, a value of $d$ = -4 was reported by Yokota et al.[33] for a scale up criterion of constant tip speed. If $d$ is negative, the value of $k_{b2,\beta}$ decreases with an increase in crystallizer size $\lambda$ and hence the solvent-mediated transformation time is prolonged (see Fig. 11). Thus, the scale up effect on the transformation time can be explained with the secondary nucleation-mediated mechanism a similar way to the stirrer speed effect.

**Implementation of the model for a real system**

The present model includes a number of parameters. Even in a dimorphic system, which is the simplest one, there are 20 parameters (see Table 1). For simulation of an actual system, these parameter values should be known *a priori*. Some of them (those of primary and secondary nucleation rates) are very difficult to predict with satisfactory accuracy at present. Recently, Kubota proposed a new model to explain metastable zone width (MSZW)[34] and he also explained MSZW and induction time[35] in a unified manner. Following this, simulation studies were performed for MSZW[36,37,38,40] and induction time.[29,32,36,38,39] In these studies, MSZW and induction time are both related to the kinetics of primary and secondary nucleations. The effects of stirrer speed, detector sensitivity and detector resolution on MSZW and induction time were explained reasonably in a unified manner. The effect of cooling rate on MSZW and the effect of supercooling on induction time were also explained. These new approaches to MSZW and induction time could be better utilized for estimation of parameters of primary and secondary nucleations. Parameters of linear crystal growth rate could be determined with experiments.[2,17] Parameters of linear dissolution rate could also be estimated.[2,15,17,28] Some other values (solid density, shape factor of crystals) are easy to estimate.

## Conclusions

In this study, a new population balance model for solvent-mediated polymorphic transformation was presented. In the model, primary nucleation and the ordinary secondary nucleation caused by nuclei grown crystals are both taken into account. This model can be extended to seeded systems with minor modification of the initial conditions. By using the model, the polymorphic solvent-mediated transformation of a hypothetical enantiotropic dimorph in an unseeded solution was simulated. In the simulation, particular attention was paid to the effect of stirrer speed on the polymorphic transformation. The effect of stirrer speed was explained with the secondary nucleation-mediated mechanism. The effect of vessel size (or scale-up) on the transformation time was also suggested to be explained with the secondary nucleation-mediated mechanism.

## Notes and references

[a] *EN Technology Center, JGC Corporation, 2-3-1 Minato Mirai, Nishi-ku, Yokohama, Japan. Fax: +81-45-682-8630; Tel: +81-45-682-8708; E-mail: kobari.masanori@jgc.co.jp*
[b] *Department of Chemistry and Bioengineering, Iwate University, 4-3-5 Ueda, Morioka, Japan. Fax: +81-42-599-5981(home); Tel: +81-42-599-5981(home); E-mail: nkubota@iwate-u.ac.jp*
[c] *Department of Applied Chemistry, School of Science and Engineering, Waseda University, 3-4-1 Okubo, Shinjuku-ku, Tokyo, Japan. Fax: +81-3-3208-6896; Tel: +81-3-5286-3215; E-mail: izumih@waseda.jp*

**Nomenclature**

$a$ empirical constant, s
$b$ empirical constant, s rpm$^{-1}$
$b1_i$ primary nucleation order of polymorph $i$ in eqn (9)
$b2_i$ secondary nucleation order of polymorph $i$ in eqn (11)
$B_{1,i}$ primary nucleation rate of polymorph $i$, s$^{-1}$ kg solvent$^{-1}$
$B_{2,i}$ secondary nucleation rate of polymorph $i$, s$^{-1}$ kg solvent$^{-1}$
$C$ concentration of solution, kg solute kg solvent$^{-1}$
$C_0$ initial concentration of solution, kg solute kg solvent$^{-1}$
$C_{sat,i}$ solution of polymorph $i$, kg solute kg solvent$^{-1}$
$d$ empirical constant in eqn (25)
$d_i$ dissolution rate order of polymorph $i$
$D_\alpha$ dissolution rate of polymorph $\alpha$, m s$^{-1}$
$g_i$ growth rate order of polymorph $i$

$G_i$ linear growth rate of crystal of polymorph $i$, m $s^{-1}$

$f_i$ dissolution factor defined by eqn (13)

$i$ index denoting polymorph α, β, .....

$j$ index denoting $j$-th moment in eqns (5) , (7) and (8) or exponent in eqn (20)

$k_{b1,i}$ primary nucleation constant of polymorph $i$ in eqn (9), $s^{-1}$ kg $solvent^{-1}$ $^oC^{-b1,i}$

$k_{b2,i}$ secondary nucleation constant of polymorph $i$ in eqn (11), $s^{-1}$ kg $solvent^{-1}$ $^oC^{-b2,i}$

$k_{d,i}$ dissolution constant of polymorph $i$, m $s^{-1}$ $^oC^{-di}$

$k_{g,i}$ linear growth rate constant of polymorph $i$ in eqn (14), $m^{-1}s$ $^oC^{-gi}$)

$k_T$ empirical constant, $s^{-1}$

$k_{v,i}$ volume shape factor of polymorph $i$

$L_i$ characteristic length of crystal of polymorph $i$, m

$L_{0,i}$ size of a nucleus born of polymorph $i$ with either primary or secondary nucleation mechanism, m

$M$ mass of solvent, kg

$n_i(L_i, t)$ population density function of polymorph $i$, $m^{-1}$ kg $solvent^{-1}$

$N_r$ agitation speed, rpm

$t$ time, s

$t_A$ time at the start of transformation, s

$t_B$ time at the end of transformation, s

$t_{trans}$ transformation time, s

$T$ temperature, $^oC$

$T_{sat,i}$ saturation temperature of polymorph $i$ at concentration $C$, $^oC$

$X_B$ solid composition of β

$\Delta T_i$ $T_{sat,i}$- $T$, supercooling of polymorph $i$, $^oC$

$\delta$ Dirac's delta function, $\delta(L\text{-}L_0) = \infty$ at $L = L_0$ and $\delta(L\text{-}L_0) = 0$ at $L \neq L_0$ with $\int_{-\infty}^{+\infty}\delta(x)dx = 1$ , $m^{-1}$

$\mu_{j,i}$ $j$-th moment of size distribution of crystals of polymorph $i$, defined by eqn (5), $m^j$ kg $solvent^{-1}$

$\mu_{3,i}(t_A)$ the third moment $\mu_{3,i}$ at $t = t_A$, s

$\lambda$ length scale of a crystallizer, m

$\theta$ elapsed time until the start of transformation , s

$\rho_{c,i}$ density of solid (crystal) of polymorph $i$, kg $m^{-3}$

## References

1 Mangin D., Puel F. and Veesler S., *Org. Process Res. Dev.*, 2009, **13**, 1241–1253.
2 Cornel J., Lindenberg C. and Mazzotti M., *Cryst. Growth Des.*, 2009, **9**, 243-252.
3 Davey R. J., Blagden N., Righini S., H. Alison H. and Ferrari E. S., *J. Phys. Chem. B*, 2002, **106**, 1954-1959.
4 Ferrari E. S. and Davey R. J., *Cryst. Growth Des.*, 2004, **4**, 1061-1068.
5 Kagara K., Machiya K., Takasuka K. and Kawai N., *Kagaku Kogaku Ronbunshu*, 1995, **21**, 437-443.
6 Maruyama S., Ooshima H. and Kato J., *Chem. Eng. J.*, 1999, **75**, 193-200.
7 Mukuta T., Lee A. Y., Kawakami T. and Myerson A. S., *Cryst. Growth Des.*, 2005, **5**, 1429-1436.
8 Yang L., Hao H., Zhou L., Chen W., Hou B., Xie C. and Yin Q., *Ind. Eng. Chem. Res*. 2013, **52**, 17667−17675.
9 Rusin M., Ewan B. C. R. and Ristic R. I., *CrystEngComm*, 2013, **15**, 2192−2196.
10 Sypek K., Burns I. S., Florence A. J. and Sefcik J., *Cryst. Growth Des*. 2012, **12**, 4821−4828.
11 Hermanto M. W., Braartz R. D. and Chiu M.-S., *AIChE J.*, 2009, **55**, 122-131.
12 Maher A., Croker D. M., Rasmuson Å. C. and Hodnett B. K., *Cryst. Growth Des*. 2012, **12**, 6151−6157.
13 Ono T., Kramer H. J. M., ter Horst J. H. and Jansens P. J., *Cryst. Growth Des.*, 2004, **4**, 1161-1167.
14 Ono T., ter Horst J. H. and Jansens P. J., *Cryst. Growth Des.*, 2004, **4**, 465-469.
15 Schöll J., Bonalumi D., Vicum L., and Mazzotti M., *Cryst. Growth Des.*, 2006, **6**, 881-891.
16 Sheikholeslamzadeh E. and Rohani S., *Ind. Eng. Chem. Res*., 2013, **52**, 2633−2641.
17 Trifkovic M., Rohani S. and Sheikhzadeh M., *Journal of Crystallization Process and Technology*, 2012, **2**, 31-43.
18 Doki N., Yokota M., Kido K., Sasaki S. and Kubota N., *Cryst. Growth Des.*, 2004, **4**. 103-107.
19 Bauer J., Spanton S., Henry R., Quick J., Dziki W., Porter W. and Morris J., *Pharm. Res*., 2001, **18**, 859-866.
20 Cardew P. T., and Davey R. J., *Proc. R. Soc. Lond.* A, 1985, **398**, 415-428.
21 Llinàs A. and Goodman J. M., *Drug Discovery Today,* 2008, **13**, 198-210.
22 Cashell C., Corcoran D. and Hodnett B. K., *ChemComm*, 2003, 374–375.
23 Wantha, L. and Flood, A. E., *Chem. Eng. & Technol*., 2013, **36**, 1313-1319.
24 Kitamura M., *J. Cryst. Growth*, 1989, **96**, 541-546.
25 Kitamura M., *CrystEngComm*, 2009, **11**, 949–964.
26 O'Mahony M. A., Seaton C. C., Croker D. M., Veesler S., Rasmuson A. C. and Hodnett B. K., *Cryst. Growth Des*. 2013, **13**, 1861−1871.
27 Ferrari, E. S., Davey, R. J.,Cross, W. I., Gillon. A.L. and Towler, C. S., *Cryst. Growth Des.*, 2003, **3**. 53-60.
28 Garside J. and Davey R. J., *Chem. Eng. Commun*, 1980, **4**, 393–424.
29 Kobari M., Kubota N. and Hirasawa I., *CrystEngComm*, 2012, **14**, 5255-5261.
30 Mullin J. W., *Crystallization*, Butterworth-Heinemann, Oxford, 4th edn, 2001.
31 Nagy Z. K., Aamir E. and Rielly C. D., *Cryst. Growth Des*. 2011, **11**, 2205–2219.
32 Kubota N., Kobari M. and Hirasawa I., *CrystEngComm*, 2014, **16**, 1103 – 1112.
33 Yokota M., Takezawa E., Takakusaki T., Sato, A., Takahashi, H. and Kubota N., *Chem. Eng. Sci.*, 1999, **54,** 3831-3838.
34 Kubota N., *J. Cryst. Growth*, 2008, **310**, 629-634.
35 Kubota N., *J. Cryst. Growth*, 2010,**312**, 548-554.
36 Kobari N., Kubota N., and Hirasawa I., *J. Cryst. Growth*, 2010,**312**, 2734-2739.
37 Kobari N., Kubota N. and Hirasawa I., *J. Cryst. Growth*, 2011,**317**, 64-69.
38 Kobari N., Kubota N. and Hirasawa I., *CrystEngComm*, 2012, **14**, 5255−5261.
39 Kobari N., Kubota N .and Hirasawa I., *CrystEngComm*, 2013, **15**, 1199 -1209.
40 Kubota N., Kobari N. and Hirasawa I, *CrystEngComm*, 2013, **15**, 2091-2098.



 